GEOLOGICAL SURVEY CIRCULAR 797

A Preliminary Study of the Santa Barbara, California, Earthquake of August 13, 1978 and its Major Aftershocks

A Preliminary Study of the Santa Barbara, California, Earthquake of August 13, 1978 and its Major Aftershocks

By W. H. K. Lee, C. E. Johnson, T. L. Henyey, and R. L. Yerkes

GEOLOGICAL SURVEY CIRCULAR 797

1978

United States Department of the Interior
CECIL D. ANDRUS, *Secretary*

Geological Survey
H. William Menard, *Director*

Library of Congress catalog-card No. 78-600153

Free on application to Branch of Distribution, U.S. Geological Survey, 1200 South Eads Street, Arlington, VA 22202

CONTENTS

ILLUSTRATIONS

TABLES

A Preliminary Study of the Santa Barbara, California, Earthquake of August 13, 1978 and its Major Aftershocks

By W. H. K. Lee, C. E. Johnson, T. L. Henyey, and R. L. Yerkes

ABSTRACT

The M_L5.1 Santa Barbara earthquake of August 13, 1978 occurred at lat 34° 22.2'N., long 119° 43.0' 4 km south of Santa Barbara, Calif. at a depth of 12.5 km in the northeast Santa Barbara Channel, part of the western Transverse Ranges geomorphic-structural province. This part of the province is characterized by seismically active, east-trending reverse faults and rates of coastal uplift that have averaged up to about 10 m/1000 years over the last 45,000 years.

No surface rupture was detected onshore. Subsurface rupture propagated northwest from the main shock toward Goleta, 15 km west of Santa Barbara, where a maximum acceleration of 0.44 *g* was measured at ground level and extensive minor damage occurred; only minor injuries were reported. A fairly well constrained fault-plane solution of the main shock and distribution of the aftershocks indicate that left-reverse-oblique slip occurred on west-northwest-trending, north-dipping reverse faults; inadequate dip control precludes good correlation with any one of several mapped faults. Had the earthquake been larger and rupture propagated to the southeast or a greater distance to the northwest, it could have posed a hazard to oil-field operations. The fault-plane solution and aftershock pattern closely fit the model of regional deformation and the solution closely resembles those of five previously mapped events located within a 15-km radius.

INTRODUCTION

A moderate-sized earthquake (M_L = 5.1, an average from five Wood-Anderson stations operated by the California Institute of Technology) occurred 4 km offshore of Santa Barbara, California at 3:54 p.m. local time (2254 GCT) on the 13th of August, 1978. Minor local damage occurred at the city of Santa Barbara; the campus of the University of California at Goleta 15 km to the west suffered extensive minor damage. Hospitals treated scores of people for minor injuries; no major injuries were reported. This report summarizes the preliminary results of our investigation of the main shock and the major aftershocks that occurred in the following five days.

The Santa Barbara Channel region is one of the most active seismic areas of California. The earliest recorded destructive earthquake, on December 21, 1812, heavily damaged several missions along the coast and had an estimated magnitude of 7. Since then, numerous events have been felt and several damaging earthquakes have occurred. In particular, almost the entire business section of Santa Barbara was destroyed or rendered unsafe by the June 29, 1925 earthquake of magnitude 6.3. Santa Barbara also was damaged by the June 30, 1941 earthquake of magnitude 6. These two earthquakes are poorly located but are inferred to have occurred very near to the August 13, 1978 event (fig. 1). A list of significant earthquakes in the Santa Barbara Channel area was prepared by Hamilton and others (1969) and later revised by Lee and Ellsworth (1975).

With increasing population along the coast and extensive petroleum development in the Santa Barbara Channel, even moderate-sized earthquakes may be hazardous. Lee and Ellsworth (1975) argued that tectonic conditions in the channel region are capable of generating an earthquake as large as magnitude 7.5. In view of the continuing likelihood that a large earthquake will occur in the Santa Barbara Channel, a major concern is the correlation of seismic data with recognized faults.

Acknowledgments.—We thank Larry Porter and Tom Wootton of the California Division of Mines and Geology and Gerry Brady of the U.S. Geological Survey for providing strong-motion data. We are grateful to Mari Gunn and Al Walter for assistance in data processing, to Bob Burford and Gary Fuis for their stimulating discussions, and to Peter Leary, John McRaney and Derek Monov for their tireless efforts in the speedy proc-

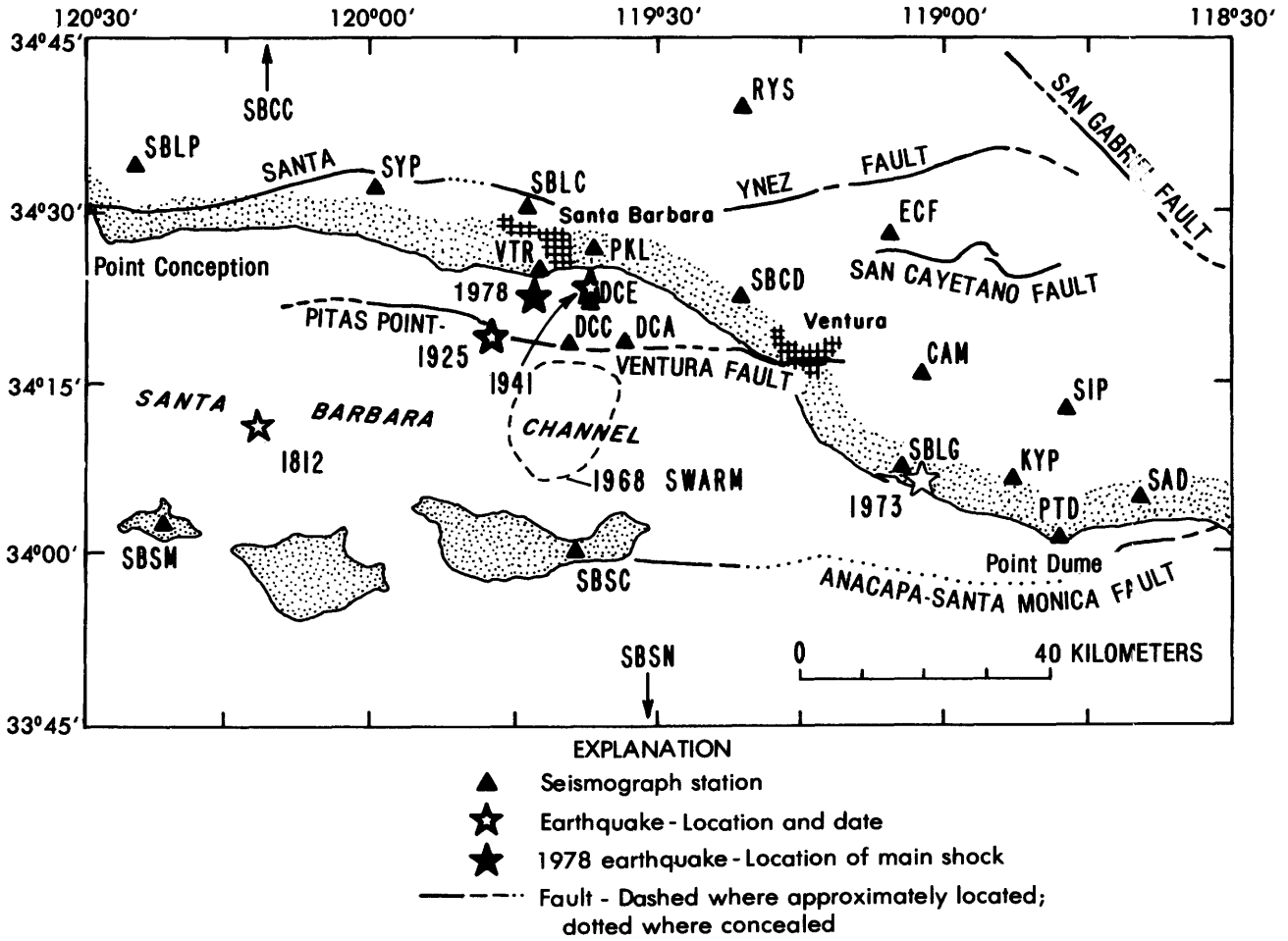

Figure 1.—Locations of principal seismograph stations and major earthquakes in Santa Barbara Channel.

essing of the USC data. The USC Santa Barbara network is supported by the Conservation Division, U.S. Geological Survey.

TECTONIC SETTING

Santa Barbara Channel occupies the southwest quarter of the western Transverse Ranges, a geomorphic-structural province of southern California. Relative to adjoining terrain, the Transverse Ranges are unique in several important respects: the distinct east-west orientation, the type, age, and history of exposed basement rocks, and the spectacular rates of compressive deformation as indicated by the imposing reverse-fault-controlled mountain fronts and the extremely deep basins filled with young, intensely deformed sediments (the Santa Barbara Channel-Ventura basin axis is coincident with the steepest known gravity gradient in California).

The western Transverse Ranges are bounded by major faults: the east-trending Santa Ynez on the north, the southeast-trending San Gabriel on the east, and the east-trending Anacapa-Santa Monica on the south. Onshore segments of each of these faults juxtapose dissimilar basement rocks: the Santa Ynez forms the south boundary of the central coast Franciscan, the San Gabriel forms the southwest boundary of exposed Precambrian anorthosites of the western San Gabriel Mountains, and the Malibu Coast-Santa Monica forms the north boundary of the western Los Angeles basin-continental borderland Franciscan terrane.

The structure of the western Transverse Ranges is dominated by east-trending reverse faults; one of the best known of these is the Red Mountain fault. Well data, geologic mapping, and several congruent fault-plane solutions show that the fault dips northward at about 60°, offsets strata as young as about 500,000 years, and has a maximum stratigraphic separation of about 7,500 m (Yeats and others, in press).

A band of moderate seismicity is associated with some of the east-trending reverse faults

within the western Transverse Ranges. This result is based on a systematic study of the 6-year (1970-1975) record of seismographic stations operated by the U.S. Geological Survey, California Institute of Technology, University of Southern California, and California Department of Water Resources (Lee and others, in press). One or more of about 200 fault-plane solutions derived from this 6-year record can be associated geometrically with segments of the Red Mountain, Pitas Point-Ventura, and San Cayentano faults, and perhaps the Mid-Channel fault and fault X (see fig. 3). The solutions show generally near-horizontal P axes oriented at an average of N. 24° E. The inferred compressive stress is reflected in earthquakes of magnitude approximately 1 to 6.5 and reverse displacement on the east-trending faults; the average slip vector indicates approximately equal parts of vertical and left-lateral slip (Yerkes and Lee, in press).

All the evidence on the rate and sense of deformation is mutually consistent for individual segments of the faults in the Santa Barbara Channel area: geologic data on the sense of latest displacement and amount and sense of stratigraphic separation, geodetic data on tilting of coastal areas underlain by the faults, uplift of dated marine terrace deposits in such areas, and associated fault-plane solutions. The average rates of uplift (up to 10 m/1000 years), indicated by dating of deposits as young as 2,500 years, show no slowing over the last 45,000 years (Yerkes and Lee, in press).

The east-trending reverse faults that dominate the structure of the western Transverse Ranges may be viewed as slip surfaces between a series of north- to northeast-dipping shingles along which many kilometers of north-south shortening and east-west extension occurred in latest Quaternary time. The Santa Barbara earthquake of 13 August 1978 and its aftershock pattern fit well with this model, and its fault-plane solution neatly fits those of five previously mapped events within 15 km of it.

DATA PROCESSING AND ANALYSIS

The Santa Barbara earthquake and its aftershocks were well recorded by the California Institute of Technology (CIT)-U.S. Geological Survey (USGS) cooperative network in southern California and by seismographic stations operated by University of Southern California (USC), University of California at Santa Barbara (UCSB), and California Department of Water Resources (DWR). It is very fortunate that the USC group established four stations (three in Santa Barbara Channel) near the epicentral area one day before the earthquake. After the earthquake, additional stations were installed by USC, USGS, and others.

In order to make a study in a short time, we selected about 100 earthquakes (out of several hundred well-recorded ones) and processed mostly data recorded at the critical stations (fig. 1). Initially, the data were processed independently at CIT, USGS, and USC. At CIT, the earthquakes were processed and analyzed in a routine manner using a computer-assisted system designed by C. E. Johnson. At USC, seismic data recorded on magnetic tapes were played back at a scale of 1 cm = 1 second and arrival times were read manually. CIT's Develocorder film recordings of SYP station (about 30 km from the epicenter) were scanned at the USGS. P-arrival, S-arrival, and signal duration were measured for events of duration 20 seconds or more. From the scan list, arrival times for the larger aftershocks were read from Develocorder films that recorded the Santa Barbara Channel region stations. Overall errors in the arrival time data are generally less than 0.1 second.

The data from these three sources were merged and analyzed. We located the earthquakes using the HYP071 computer program (Lee and Lahr, 1975). Initially, we used Healy's (1963) crustal structure model and station delays worked out for the Western Transverse Ranges by Lee, Yerkes, and Simirenko (in press). This allowed us to eliminate gross errors in arrival times quickly. We then selected 17 well-recorded earthquakes and derived a set of station corrections using a crustal model (fig. 2) which approximates a tentative velocity profile in Santa Barbara Channel obtained from a geophysical survey using the seismic-reflection method.

Station coordinates and station delays are given in table 1. Finally, we relocated all earthquakes using this crustal model and the station delays. Earthquakes were located on the basis of P-wave arrival times. The HYP071 computer program employs Geiger's (1912) method to determine hypocenters by minimizing the residuals between observed and calculated arrivals. Travel times from a trial hypocenter to the stations and their partial derivatives are computed on the assumption of a horizontal multilayer model by a technique introduced by Eaton (1969). Earthquake magnitudes were estimated using the signal duration method (Lee and others, 1972). However, the present earthquake magnitude estimates are very crude and should be calibrated against the local magnitude scale originally proposed by Richter in 1935 (Richter, 1958). For example, magnitude estimated from signal duration for the main shock (table 2) is 4.9, whereas the average Richter magnitude of five Wood-Anderson stations is 5.1.

DISTRIBUTION OF HYPOCENTERS

A total of 71 earthquakes that occurred from 2254 GCT August 13 to 0718 GCT August 18, 1978 are listed chronologically in table 2. Included are the origin time, location of hypocenter (epicenter and focal depth), magnitude, and number of arrival times used. In addition, five parameters are listed as a means of evaluating the quality of the hypocenter solution:

Table 1.— *Coordinates and delays of principal seismographic stations used in the present study*

Station code	Latitude (N)	Longitude (W)	Elevation (m)	Delay (s)
DCA	34° 18.72'	119° 33.68'	-76	0.28
DCC	34° 18.57'	119° 39.35'	-82	.34
DCE	34° 22.00'	119° 37.35'	-46	.04
PKL	34° 26.84'	119° 36.98'	142	- .39
VTR	34° 24.32'	119° 42.85'	122	0.00
SBCC	34° 56.48'	120° 10.32'	610	.72
SBCD	34° 22.12'	119° 20.63'	213	.04
SBLC	34° 29.79'	119° 42.81'	1190	- .33
SBLG	34° 6.57'	119° 3.85'	415	- .77
SBLP	34° 33.62'	120° 24.03'	134	.29
SBSC	33° 59.68'	119° 37.99'	457	- .59
SBSM	34° 2.25'	120° 20.99'	172	- .19
SBSN*	33° 14.70'	119° 30.40'	259	--
CAM	34° 15.27'	119° 1.99'	271	.29
ECF	34° 27.48'	119° 5.44'	1005	.17
KYP*	34° 6.10'	118° 52.77'	701	--
PTD*	34° 0.25'	118° 48.37'	41	--
SAD*	34° 4.88'	118° 39.90'	727	--
SIP*	34° 12.26'	118° 46.92'	701	--
SYP	34° 31.60'	119° 58.70'	1305	.02

*These stations are located more than 80 km from the Santa Barbara earthquakes and were not used in the earthquake location.

(1) the largest azimuthal separation between stations (α), (2) epicentral distance to the nearest station (β), (3) root-mean-square error of the time residuals, (4) standard error of the epicenter, and (5) standard error of the focal depth. On the basis of these parameters, the general reliability of each earthquake solution is graded as either excellent (A), good (B), fair (C), or poor (D). The criteria for these classifications are given in table 3.

A brief discussion of the accuracy of hypocenter solution of earthquakes was given by Lee, Eaton, and Brabb (1971). To obtain a reliable epicenter, the largest azimuthal separation between stations (α) should be less than 180°, so that the earthquake epicenter is surrounded by stations. To obtain a reliable focal depth, epicentral distance to the nearest station (β) should be less than the focal depth, so that there is a direct ray-path. In addition, systematic errors arise from uncertainties in the crustal velocity model. These errors cannot be determined without controlled experiments, such as calibrated explosions in the focal region. Owing to the irregular distribution of stations and occasional loss of data from critical stations, the quality of hypocenter solutions in table 2 varies. Although standard errors of epicenters and focal depth are given, they must be interpreted with caution, especially for quality C and D solutions. These standard errors are computed with respect to the assumed crustal velocity model, which is not necessarily a good approximation to the real earth.

The epicenter distribution (fig. 3) shows a linear trend of N. 60° W. with the main shock at the southeastern end. The dimension of the immediate aftershock area is approximately 3 by 12 km. The main shock was preceded four hours by a small earthquake located at the lower right-hand corner of the area of figure 3. It is not clear to us whether this earthquake is related to the Santa Barbara earthquake. However, it occurred in an area where a swarm of earthquakes took place in March and April of 1978. Immediately after the main shock, seismic activity was

concentrated 7 km northwest of the main event. Later, a few aftershocks occurred nearer to the main shock; only two aftershocks located southeast of the main shock occurred in the first five days. On August 16 a few earthquakes occurred 10 km south of the epicenter; they appear to be associated with a different fault.

LOCATION OF THE MAIN SHOCK

We are fortunate that the Santa Barbara earthquakes were surrounded by seismograph stations and especially that three stations were within 10 km of the earthquake epicenters (see fig. 1). However, most of the stations are located northeast of the earthquakes. To lessen the station-distribution bias, we employed azimuthal weighting (Lee and Lahr, 1975), ignored stations farther than 80 km from the earthquake location, and also assigned greater weights to stations within 40 km of the earthquakes.

The biggest uncertainty in earthquake location is due to our lack of knowledge of the crustal structure under the Santa Barbara Channel region. Experiments with various crustal models indicate that the epicenter error may be as high as ±3 km and the focal-depth error ±5 km. For a given crustal model, we also experimented with different subsets of arrival-time data for the main shock. The results showed that (1) epicentral locations do not differ more than ±1 km if the earthquake is surrounded (maximum azimuthal gap between stations less than 180°), and (2) focal depths do not differ more than ±2 km if there is a station within 10 km of the earthquake. The relative location errors between different earthquakes are small because we use station corrections derived from a set of better recorded earthquakes.

In view of the above discussion, we suggest the following main-shock parameters:

Origin time = $22^h\ 54^m\ 52.4^s$ (±0.1 s)

Epicenter = 34° 22.2' N., 119° 43.0' W. (±2 km)

Focal depth = 12.5 km (±3 km)

Magnitude = M_L = 5.1 (average of five CIT Wood-Anderson stations)

The location parameters are also supported by the strong-motion data obtained from both the USGS and the California Division of Mines and Geology (CDMG). The time interval between S-wave arrival and the initiation of recording at the accelerometer (S-trigger time) is a minimum estimate of the S-P interval because the recorder may not be triggered by the first P-wave arrival. If we adopt our main-shock location and a ratio of P-velocity to S-velocity of 1.7, we obtain the following differences between computed S-P and observed S-trigger times:

Strong-motion station	Maximum acceleration	Trigger time	Computed S-P time	Difference
Santa Barbara Court House (USGS)	0.21*g*	1.9s	2.4s	-0.5s
Univ. Calif. Santa Barbara North Hall (CDMG)	0.44*g*	3.1s	3.0s	+0.1s
Goleta Free-field (CDMG)	0.37*g*	3.3s	3.7s	-0.4s

These time differences indicate that our main-shock location and its error estimates are reasonable. In addition, the station SBC (at

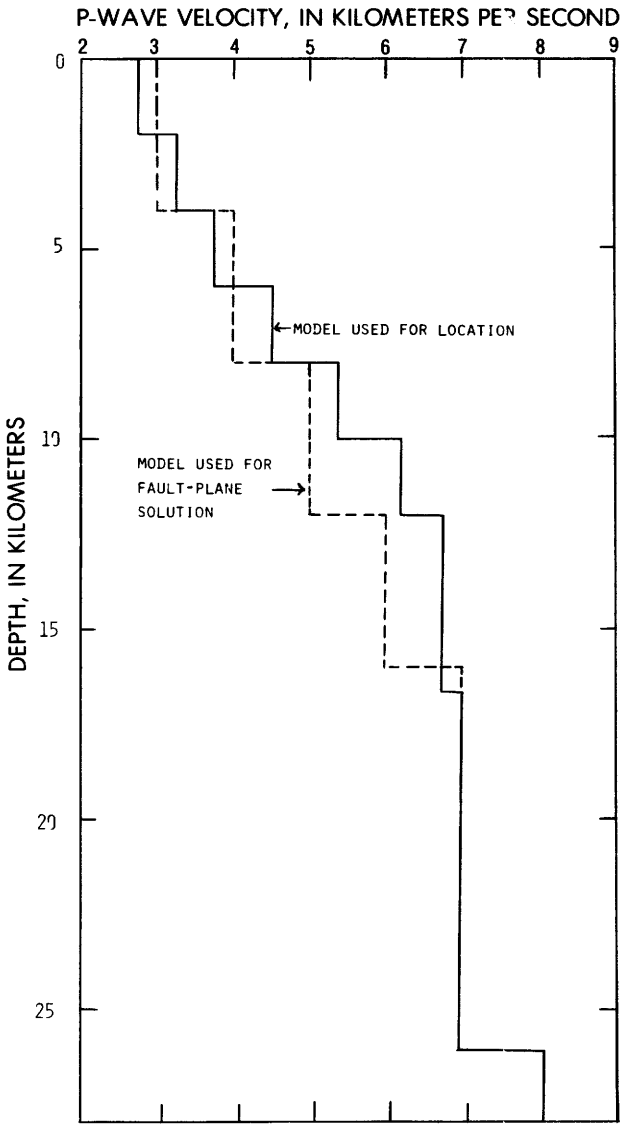

Figure 2.—Crustal structure models.

Table 2.—*List of Santa Barbara earthquakes, August 13-18, 1978*

[YEAR, MON, DAY, HR, MN, SEC, origin time in Greenwich Civil Time (GCT). LAT N, LONG W, location of epicenter in degrees and minutes of north latitude and west longitude. DEPTH, depth of focus in kilometers. MAG, local magnitude (M_L) of the earthquake estimated from signal durations. NO, number of stations used in locating earthquake. GAP, largest azimuthal separation in degrees between stations. DMIN, epicentral distance in kilometers to the nearest station. RMS, root-mean-square error of the time residuals: $RMS = [\Sigma_i (R_i^2/NO]^{\frac{1}{2}}$, where R_i is the observed seismic-wave arrival time minus the computed time at the ith station. ERH, standard error of the epicenter in kilometers: $ERH = [SDX^2 + SDY^2]^{\frac{1}{2}}$. *SDX* and *SDY* are the standard errors in latitude and longitude, respectively, of the epicenter. When *NO* <5, *ERH* cannot be computed and is left blank. ERZ, standard error of the focal depth in kilometers. When *NO* <5, *ERZ* cannot be computed and is left blank. If *ERZ* ≥ 20 km, it is also left blank. Q, solution quality of the hypometer (table 3)]

EVENT	YEAR	MON	DY	HR	MN	SEC	LAT N	LONG W	DEPTH	MAG	NO	GAP	DMIN	RMS	ERH	ERZ	Q
1	1978	AUG	13	22	54	52.4	34-22.1	119-42.9	12.5	4.9	16	68	4.0	0.05	0.2	0.4	A
2			13	23	1	0.7	34-24.2	119-46.3	12.9	2.4	11	98	5.3	0.03	0.3	0.2	B
3			13	23	1	32.4	34-24.8	119-48.2	11.9	2.1	8	228	8.2	0.10	2.2	0.8	C
4			13	23	2	45.6	34-24.4	119-46.2	12.7	2.7	11	68	5.2	0.05	0.4	0.5	A
5			13	23	4	13.9	34-23.8	119-45.7	12.0	2.5	5	193	4.5	0.00	0.2	0.1	C
6			13	23	5	1.4	34-23.1	119-47.6	9.1	2.4	10	128	7.7	0.06	0.5	0.5	B
7			13	23	6	19.0	34-24.3	119-46.3	12.5	2.1	14	68	5.3	0.05	0.3	0.6	A
8			13	23	6	57.4	34-24.9	119-46.5	12.1	1.9	9	124	5.7	0.04	0.5	0.7	B
9			13	23	7	30.1	34-24.6	119-46.6	12.2	2.7	13	70	5.8	0.03	0.2	0.4	A
10			13	23	8	27.1	34-24.3	119-46.6	12.4	3.1	13	69	11.7	0.05	0.2	1.3	A
11			13	23	9	20.9	34-24.7	119-45.9	12.1	2.5	8	122	4.7	0.04	0.5	0.6	B
12			13	23	10	9.3	34-24.4	119-48.3	11.3	2.6	9	126	8.4	0.02	0.1	0.2	B
13			13	23	11	1.7	34-24.3	119-46.4	12.8	3.3	12	123	5.5	0.02	0.1	0.3	B
14			13	23	15	2.5	34-24.4	119-46.4	12.6	3.0	16	68	5.4	0.11	0.5	1.1	A
15			13	23	16	42.4	34-24.4	119-45.3	11.3	2.1	11	70	3.8	0.05	0.3	0.3	A
16			13	23	18	10.1	34-22.9	119-43.7	13.4	2.3	13	96	2.9	0.06	0.4	0.4	B
17			13	23	18	32.0	34-25.5	119-36.2	0.3	2.1	6	96	10.4	0.15	1.5	2.3	C
18			13	23	18	56.9	34-23.5	119-44.9	13.1	2.9	12	97	3.4	0.03	0.2	0.3	B
19			13	23	19	42.4	34-24.0	119-44.2	11.5	1.7	8	125	2.1	0.10	1.3	0.7	B
20			13	23	22	50.6	34-23.3	119-43.2	14.3	2.1	8	115	2.0	0.02	0.2	0.2	B
21			13	23	23	25.9	34-24.7	119-47.1	12.2	3.0	12	98	6.6	0.02	0.1	0.3	B
22			13	23	23	53.8	34-24.0	119-44.7	12.5	2.9	9	146	2.9	0.01	0.1	0.2	B
23			13	23	30	46.8	34-24.8	119-49.0	10.7	2.0	12	81	9.5	0.05	0.3	0.4	A
24			13	23	31	44.9	34-22.9	119-43.1	13.1	2.0	9	114	2.6	0.02	0.2	0.2	B
25			13	23	34	26.5	34-24.6	119-47.2	13.6	2.3	9	75	6.7	0.04	0.3	0.5	A
26			13	23	35	53.7	34-24.4	119-46.6	12.7	2.3	12	73	5.8	0.08	0.5	0.8	A
27			13	23	40	2.5	34-24.8	119-47.5	10.6	2.6	13	75	11.7	0.08	0.4	0.7	B
28			13	23	52	16.5	34-23.2	119-43.9	10.9	2.0	10	163	2.6	0.04	0.3	0.3	B
29			13	23	54	52.3	34-24.7	119-48.9	11.2	2.9	15	70	9.4	0.04	0.2	0.3	A
30			13	23	56	3.0	34-24.5	119-48.3	9.8	3.1	13	70	12.9	0.06	0.3	2.4	B

EVENT	YEAR	MON	DY	HR	MN	SEC	LAT N	LONG W	DEPTH	MAG	NO	GAP	DMIN	RMS	ERH	ERZ	Q
31			14	0	14	1.3	34-24.0	119-47.3	11.4	2.3	14	70	6.9	0.03	0.2	0.2	A
32			14	0	21	13.5	34-24.8	119-48.8	11.1	2.9	13	127	9.1	0.03	0.2	0.2	B
33			14	0	36	43.6	34-24.0	119-47.3	12.4	2.6	14	70	6.8	0.04	0.2	0.6	A
34			14	0	40	10.9	34-24.2	119-46.6	12.8	2.3	10	99	5.7	0.03	0.2	0.4	B
35			14	1	2	35.1	34-23.9	119-43.1	14.1	2.7	15	65	0.9	0.03	0.1	0.2	A
36			14	1	18	58.6	34-24.6	119-47.6	12.6	2.2	15	69	7.3	0.04	0.2	0.4	A
37			14	1	24	4.1	34-20.6	119-43.4	9.8	2.4	14	72	6.9	0.06	0.3	0.2	A
38			14	2	5	19.2	34-23.7	119-46.8	12.5	1.9	13	70	6.2	0.05	0.3	0.6	A
39			14	2	28	56.9	34-23.7	119-45.5	13.3	2.4	16	68	4.2	0.02	0.1	0.2	A
40			14	4	0	52.9	34-23.6	119-44.6	13.4	2.4	16	68	2.9	0.03	0.2	0.2	A
41			14	5	9	40.5	34-23.6	119-44.4	13.5	2.2	15	67	2.7	0.02	0.1	0.2	A
42			14	5	22	42.1	34-23.4	119-43.2	13.3	2.7	13	133	1.7	0.05	0.3	0.4	B
43			14	6	33	26.8	34-24.1	119-44.3	13.5	2.1	15	66	2.2	0.04	0.2	0.3	A
44			14	7	1	18.6	34-24.6	119-45.1	10.0	2.4	14	67	3.5	0.10	0.5	0.4	A
45			14	7	3	15.3	34-23.8	119-45.4	13.2	2.2	14	68	4.0	0.03	0.1	0.2	A
46			14	7	45	50.6	34-24.5	119-48.3	11.3	2.3	14	70	8.4	0.04	0.3	0.4	A
47			14	7	47	54.7	34-25.0	119-47.4	13.9	2.0	13	68	7.2	0.01	0.1	0.1	A
48			14	8	46	51.3	34-24.2	119-47.4	10.9	3.2	13	70	7.0	0.09	0.6	0.7	A
49			14	12	53	42.0	34-24.4	119-46.5	13.5	2.4	5	171	5.6	0.25	11.2	10.0	D
50			14	16	7	25.3	34-23.9	119-45.5	13.7	2.5	13	68	4.1	0.04	0.3	0.4	A
51			14	16	55	0.5	34-19.4	119-49.7	14.5	2.3	9	83	13.9	0.08	0.8	3.1	B
52			14	17	25	56.4	34-19.4	119-50.4	9.0	2.3	9	95	14.8	0.11	0.8	1.1	B
53			15	4	37	12.5	34-20.1	119-50.6	6.9	2.4	10	135	14.2	0.05	0.3	0.4	B
54			15	6	25	56.8	34-20.1	119-50.7	6.5	2.3	11	95	14.4	0.07	0.4	0.8	B
55			15	9	58	32.1	34-25.0	119-47.1	11.8	2.3	5	185	6.7	0.06	0.2	0.0	C
56			15	15	52	45.5	34-23.1	119-48.4	11.1	2.1	6	194	8.8	0.12	4.1	2.8	D
57			15	17	16	42.8	34-23.7	119-44.6	13.9	2.3	9	139	3.0	0.02	0.3	0.3	B
58			16	0	39	33.8	34-23.8	119-45.3	12.3	2.3	8	98	3.9	0.06	0.6	0.9	B
59			16	4	24	29.4	34-21.9	119-42.6	11.6	2.3	10	68	4.4	0.06	0.4	0.3	A
60			16	5	31	6.0	34-15.8	119-43.7	7.7	2.5	11	92	8.5	0.04	0.3	0.3	B
61			16	7	43	34.8	34-24.2	119-46.8	12.7	2.1	12	75	6.1	0.05	0.3	0.6	A
62			16	8	57	56.7	34-19.7	119-49.6	8.0	2.3	11	91	13.4	0.07	0.3	0.7	B
63			16	9	57	28.5	34-21.9	119-42.5	10.9	2.4	13	68	4.5	0.06	0.4	0.3	A
64			16	10	43	37.4	34-23.8	119-45.4	12.8	2.1	11	71	3.9	0.03	0.2	0.3	A
65			16	11	40	27.9	34-23.6	119-45.7	11.8	2.8	14	69	4.6	0.04	0.2	0.2	A
66			16	13	35	11.6	34-24.6	119-48.3	11.5	3.2	15	71	8.3	0.06	0.3	0.4	A
67			17	2	58	6.0	34-23.9	119-48.8	13.8	2.6	13	71	9.1	0.14	0.7	1.6	A
68			17	12	52	8.0	34-24.4	119-46.3	13.5	2.1	5	170	5.3	0.15	6.4	5.7	D
69			18	1	55	6.0	34-24.5	119-47.7	12.0	2.1	11	69	7.5	0.04	0.2	0.5	A
70			18	2	24	21.8	34-24.6	119-46.4	13.7	1.9	6	169	5.5	0.03	0.5	0.8	B
71			18	7	18	51.4	34-24.1	119-46.0	12.6	2.1	12	68	4.8	0.06	0.5	0.7	A

Table 3.—*Criteria for the four quality grades of* Q

[Q is based on both the nature of the station distribution with respect to the earthquake and the statistical measure of the solution. These two factors are each rated independently. Q is taken as the average of the ratings from the two schemes, for example, an A and a C yield a B, and two B's yield a B. When the two ratings are only one level apart the lower one is used; for example, an A and a B yield a B]

	Solution quality		Station distribution			Statistical measures		
Q	Epicenter	Focal depth	NO	GAP	DMIN	RMS	ERH	ERZ
A	Excellent--------Good----		> 5	90°	≦ Depth or 5 km	< 0.15 s	< 1.0 km	< 2.0 km
B	Good----------Fair----		> 5	135°	≦ 2 x depth or 10 km	< 0.30	< 2.5	< 5.0
C	Fair----------Poor----		> 5	180°	≦ 50 km	< 0.50	< 5.0	> 5.0
D	Poor----------Poor----		< 5	180°	> 50 km	> 0.50	> 5.0	> 5.0

Santa Barbara Museum of Natural History and operated by CIT) gives S-P time of 2.0 s from its torsion and strong-motion instruments. If we include the SBC data and the above S-trigger times as S-P intervals in our location of the main shock, the epicenter differs by about 1 km and the focal depth by about 2 km from our preferred location.

FOCAL MECHANISM OF THE MAIN SHOCK

Fault-plane solutions of an earthquake can be determined directly from the first-motion pattern of P-waves provided that (1) the earthquake is well located, (2) the emergent angles

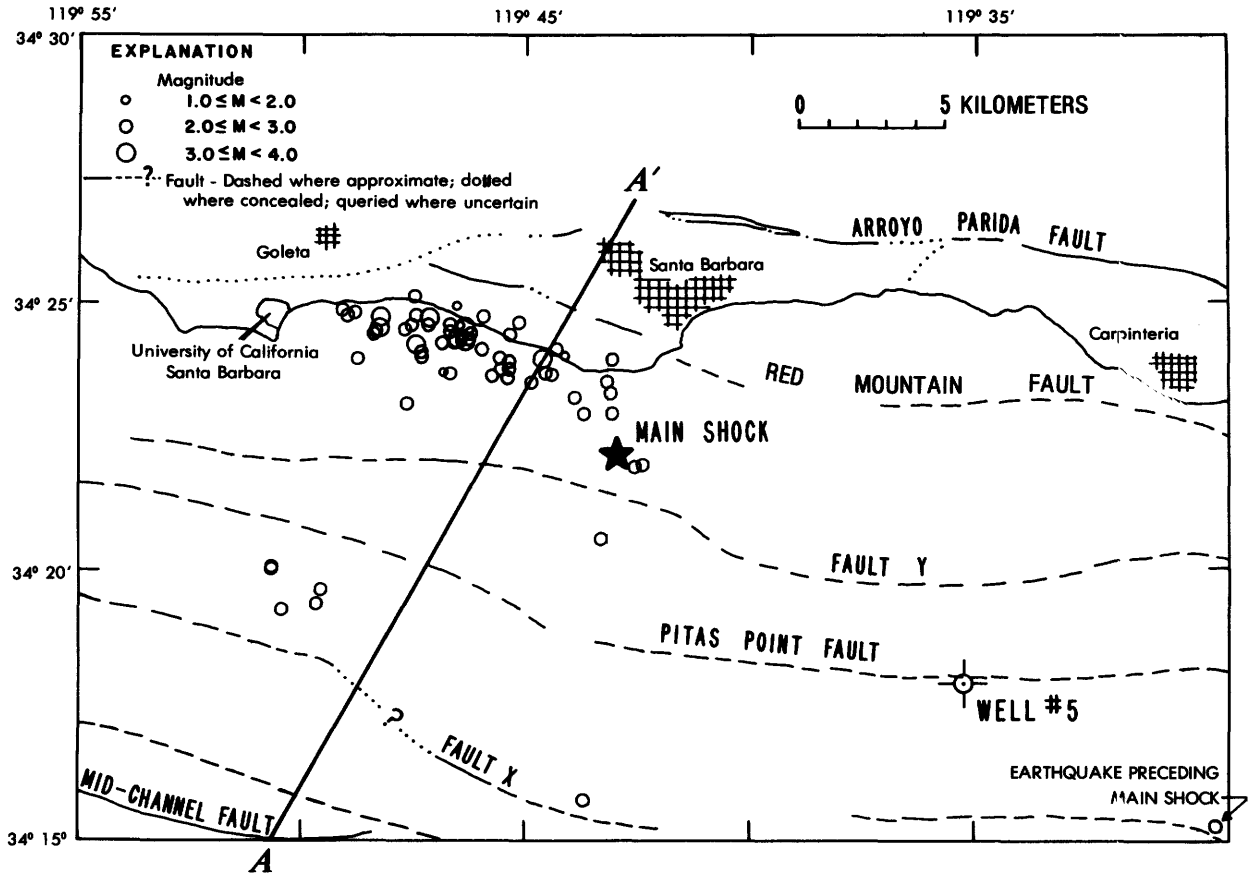

Figure 3.—Epicenters of Santa Barbara earthquake and its major aftershocks.

of seismic waves to the stations are computed correctly from an adequate crustal model, and (3) the true polarity of the first P-motions is properly identified from seismograms. The model we used to locate the earthquakes approximates the travel times well, but it has too many arbitrarily discrete layers. Consequently, it may give an erroneous first-motion pattern. Therefore, we used a simpler crustal model (see fig. 2) for computing the first-motion pattern. Figure 4 shows our fault-plane solution of the main shock. The two possible fault planes are (1) strike N. 66° W., dip 40° N., and (2) strike N. 22° W., dip 60° S. The focal mechanism indicates reverse faulting with a minor strike-slip component. The local geology and spatial distribution of the aftershocks obviously favor the N. 66 W. -40° N. fault plane, which has a minor left-lateral component. Our poor knowledge of the crustal structure precludes determination of the dip to better than ±10°. The strike of the north-dipping fault plane is reasonably well constrained, but that of the south-dipping plane is poorly constrained. If, as in the present case, we interpret the crustal structure in terms of a simple multilayer model, then the dip of the fault plane is controlled by the first critical refraction angle of seismic rays to the intermediate-distance stations. This in turn depends on the velocity contrast between the rocks in the focal area and those immediately below. The fault dip (ϕ) is determined approximately by:

$$\phi \cong 90° - \sin^{-1} (v_1/v_2)$$

where v_1 is the layer velocity containing the earthquake focus and v_2 is the velocity of the layer next below. It is unlikely that the dip will be larger than 60° because that would require v_2 to be more than twice v_1, which is unlikely because v_2 cannot be greater than 8 km/s in the lower crust, and v_1 is probably not less than 4 km/s at a depth of 12 km.

CORRELATION

In an attempt to identify the fault or faults that generated the August 13, 1978 earthquake, we plotted a cross section of the earthquake hypocenters along line A-A' (fig. 3), which is perpendicular to the trend of the aftershock pattern. The result is shown in figure 5. The present data are inadequate to uniquely identify the generative fault. First, the fault may not be a uniformly dipping surface. Second, the hypocenters could be fitted to a surface dipping between 30° and 75° N. The fault-plane solution of the main shock suggests that faulting occurred on a plane dipping about 40° N. but not greater than 60° N.; if that plane is projected to the surface it can be correlated with fault X. However, geologic data in the eastern Santa Barbara Channel indicate that some structural features south of well number 5 (fig. 3) dip south. The Pitas Point fault dips steeply north near the surface and could be the generative fault if it dips more gently at depth.

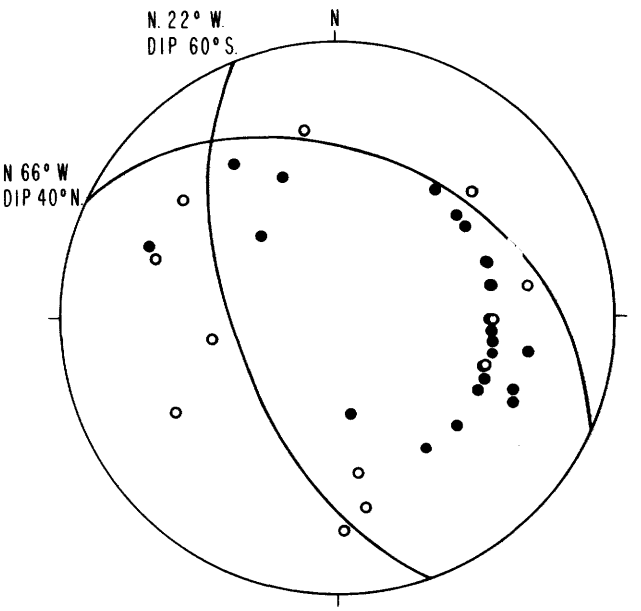

Figure 4.—Fault-plane solution of Santa Barbara earthquake.

CONCLUSIONS

Preliminary results on the Santa Barbara earthquake and its major aftershocks indicate that reverse faulting took place on a north-dipping fault at a depth of about 12 km and that the rupture propagated northwest toward Goleta. This is consistent with 0.44*g* maximum acceleration recorded by CDMG in Goleta at North Hall, University of California at Santa Barbara; most of the damage occurred in Goleta also. In addition, extension of the trend of the aftershock pattern westward intersects the shoreline at the mouth of Telecote Canyon; severe shaking there caused failure of a long segment of unsupported railroad fill and the resulting derailment and wreck of a freight train about 7 minutes after the earthquake.

The Santa Barbara earthquake was relatively small, and there was no onshore surface rupture. The subsurface rupture progagated to the northwest. Had the earthquake been larger and rupture propagated to the southeast or a greater distance to the northwest, it could have posed a hazard to oilfield operations. It is interesting to note that the June 30, 1941 Santa Barbara earthquake was preceded by an earthquake swarm in February of 1941. Similarly, the August 13, 1978 Santa Barbara earthquake was preceded by an earthquake swarm located about 20 km toward the southeast in March and April of 1978. Ten years before, the 1968 earthquake swarm in

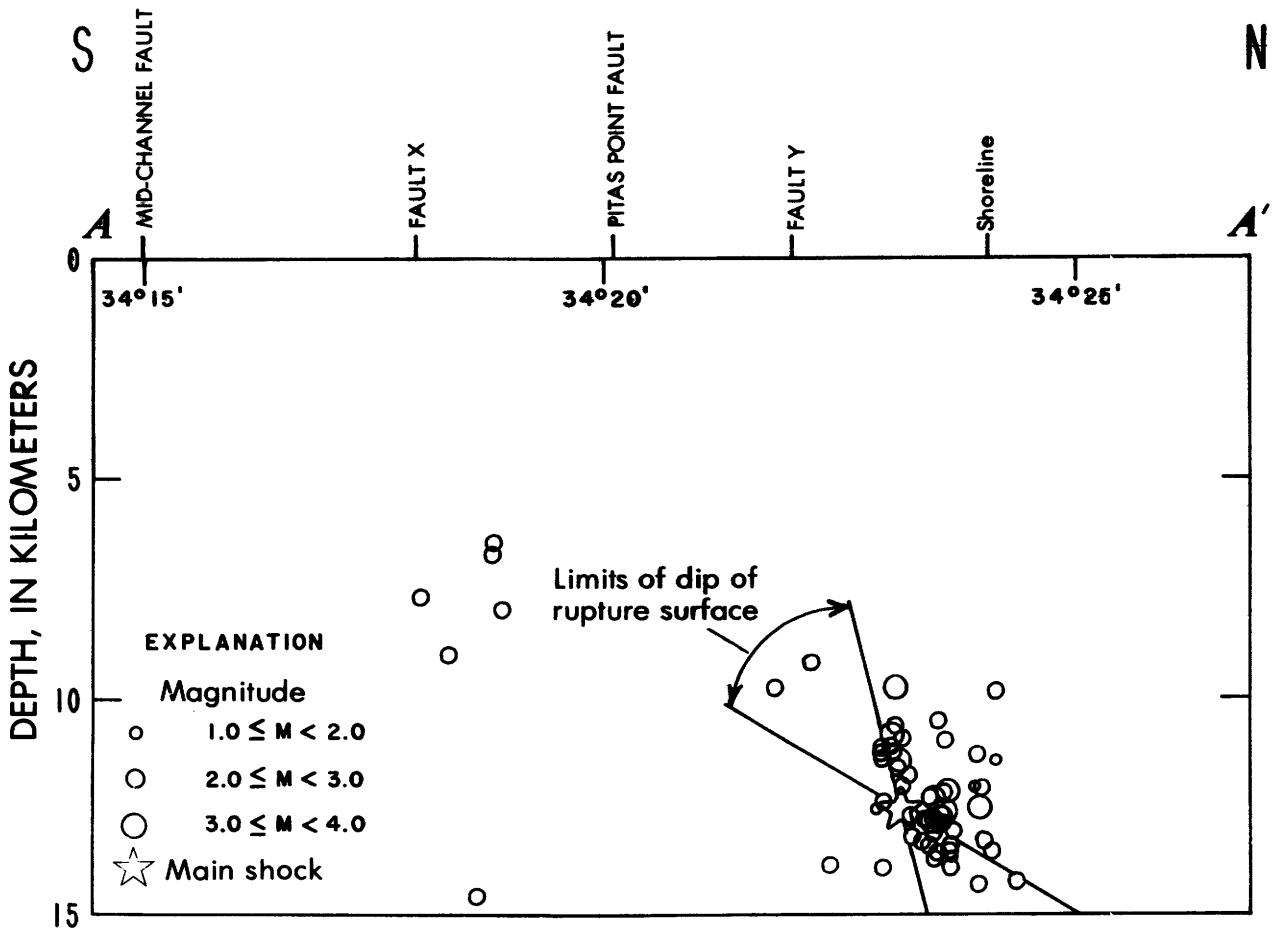

Figure 5.—Cross section of area of figure 3, showing hypocenter distributions and faults.

the Santa Barbara Channel was located in the same general area as the March-April 1978 swarm and included a magnitude 5.2 event (fig. 1) (Sylvester and others, 1970). However, this swarm was not followed by any larger earthquake. Therefore, it is not clear that earthquake swarms are reliable precursors to larger earthquakes in the Santa Barbara Channel.

REFERENCES CITED

Allen, C. R., St. Amand, P., Richter, C. F., and Nordquist, J. M., 1965, Relationship between seismicity and geologic structure in the southern California region: Seismol. Soc. America Bull., v. 55, p. 753-797.

Eaton, J. P., 1969, Hypolayer—a computer program for determining hypocenters of local earthquakes in an earth consisting of uniform flat layers over a half-space: U.S. Geol. Survey open-file report, 155 p.

Ellsworth, W. L., Campbell, R. H., Hill, D. P., Page, R. A., Alewine, R. W., III, Hanks, T. C., Heaton, T. H., Hileman, J. A., Kanamori, H., Minster, B., and Whitcomb, J. H., 1973, Point Mugu, California, earthquake of 21 February, 1973, and its aftershocks: Science, v. 182, p. 1127-1129.

Geiger, L., 1912, Probability method for the determination of earthquake epicenters from the arrival time only (translated from Geiger's 1910 German article): Bull. St. Louis Univ., v. 8, p. 56-71.

Hamilton, R. M., Yerkes, R. F., Brown, R. D., Jr., Burford, R. O., and De Noyer, J. M., 1969, Seismicity and associated effects, Santa Barbara region, pt. D of Geology, petroleum development, and seismicity of the Santa Barbara Channel region, California: U.S. Geol. Survey Prof. Paper 679, p. 47-68.

Healy, J. H., 1963, Crustal structure along the coast of California from seismic refraction measurements: J. Geophys. Res., v. 68, p. 5777-5787.

Hileman, J. A., Allen, C. R., and Nordquist, J. M., 1973, Seismicity of the southern California region: Contribution no. 2385, Div. of Geological and Planetary Sciences, California Institute of Technology.

Lee, W. H. K., Bennett, R. E., and Meagher, K. L., 1972, A method of estimating magnitude of local earthquakes from signal duration: U.S. Geological Survey open-file report, 28 p.

Lee, W. H. K., Eaton, M. S., and Brabb, E. E., 1971, The earthquake sequence near Danville,

California, 1970: Seismological Society of America Bulletin, v. 61, p. 1771-1794.

Lee, W. H. K., and Ellsworth, W. L., 1975, Earthquake activity in the Santa Barbara Channel region, in Draft environment statement, Oil and gas development in the Santa Barbara Channel outer continental shelf off California: U.S. Geological Survey, p. II-80 - II-137.

Lee, W. H. K., and Lahr, J. C., 1975, HYPO71 (Revised): A computer program for determining hypocenter, magnitude, and first motion pattern of local earthquakes: U.S. Geological Survey Open-file Report 75-311, 114 p.

Lee, W. H. K., Yerkes, R. F., and Simirenko, M., (in press), Recent earthquake activity and focal mechanisms in the western Transverse Ranges, California: U.S. Geological Survey Circular 799A.

Richter, C. F., 1958, Elementary seismology: San Francisco, W. H. Freedman and Company, 768 p.

Stierman, D. J., and Ellsworth, W. L., 1976, Aftershocks of the February 21, 1973 Point Mugu, California earthquake: Seismological Society of America Bulletin, v. 66, no. 6, p. 1931-1952.

Sylvester, A. G., Smith, S. W., and Scholz, C. H., 1970, Earthquake swarm in the Santa Barbara Channel, California, 1968: Seismological Society of America Bulletin, v. 60, p. 1047-1060.

Yeats, R. S., Lee, W. H. K., and Yerkes, R. F., (in press), Geology and seismicity of the eastern end of the Red Mountain fault, Ventura County, California: U.S. Geological Survey Professional Paper.

Yerkes, R. F., and Lee, W. H. K., (in press), Late Quaternary deformation in the western Transverse Ranges, California: U.S. Geological Survey Circular 799B.

☆ U.S. GOVERNMENT PRINTING OFFICE : 1978 689—035/48